[7] C. Cu, H. Rohdin, and C. Stolte, "1/f noise in GaAs MESFETs," in *IEEE IEDM Dig.*, 1983, p. 601.
[8] A. der Ziel, "Noise in solid state devices," *Advances Electron. and Electron Phys.*, vol. 46, p. 313, 1978.
[9] A. H. Pawlikiewicz and A. der Ziel, "Location of 1/f noise sources in BJT's—II: Experiment," *IEEE Trans. Electron Devices*, vol. ED-34, p. 2009, Sept. 1987.
[10] B Hughes, N G. Fernandez, and J. M. Gladstone, "GaAs FET's with a flicker-noise corner below 1 MHz," *IEEE Trans Electron Devices*, vol. ED-34, p. 733, Apr. 1987.
[11] I. Banerjee, P W Chye, and P. E. Gregory, "Unusual C–V profiles of Si-implanted (211) GaAs substrates and unusually low-noise MESFET's fabricated on them," *IEEE Electron Device Lett.*, vol. 9, p. 10, Jan. 1988.
[12] N. Hayama, A. Okamoto, M. Madihian, and K. Honjo, "Submicrometer fully self-aligned AlGaAs/GaAs heterojunction bipolar transistor," *IEEE Electron Device Lett.*, vol. EDL-8, p. 246, May 1987.
[13] S. R. LeSage, M. Madihian, N. Hayama, and K. Honjo, "15.6 GHz HBT microstrip oscillator," *Electron Lett.*, vol. 24, p. 230, 18 Feb. 1988.
[14] J. Sone and Y. Takayama, "A 7 GHz common-drain GaAs FET oscillator stabilized with a dielectric resonator," *IECE Japan*, vol. MW-77, p. 59, 1977.
[15] G. Pataut and D. Pavlidis, "X-band varactor tuned monolithic GaAs FET oscillators," *Int J Electron.*, vol. 64, p. 731, 1988.
[16] P. C Wade, "X-band reverse channel GaAs FET power VCO," *Microwave J.*, p. 92, Apr. 1978.
[17] F. N. Sechi and J. E. Brown, "Ku-band FET oscillator," in *IEEE Int. Solid-State Circuits Conf. Dig.*, 1980, p. 124.
[18] M. E. Kim *et al.*, "12–40 GHz low harmonic distortion and phase noise performance of GaAs heterojunction bipolar transistors," presented at the 1988 IEEE GaAs IC Symp., Nashville, TN, 1988.

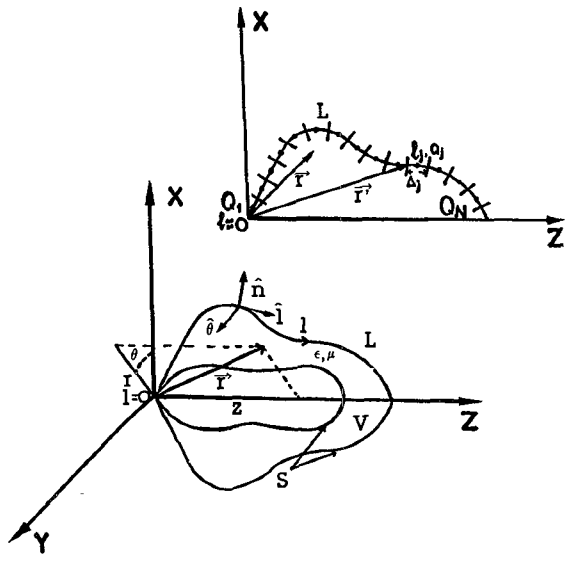

Fig. 1. Geometry and cylindrical coordinates for a body of revolution and the orthogonal right-handed triad of unit vectors n, θ, l defined within the boundary. Discretization of generating arc for body of revolution.

Integral Numerical Technique for the Study of Axially Symmetric Resonant Devices

J. RUIZ, M. J. NÚÑEZ, A. NAVARRO, AND E. MARTÍN, MEMBER, IEEE

***Abstract*—A numerical technique is proposed which is based on the coupling of Kirchhoff's integral formulation and the moment method and is suitable for application to the study of a wide class of axially symmetric resonant devices. Numerical results are presented and compared with corresponding theoretical data for two systems which allow an analytical treatment. In this way the validity of method has been confirmed.**

I. Introduction

This paper presents a numerical technique which is based on Kirchhoff's integral formulation for the electromagnetic field and which is valid for the study of a wide class of axially symmetric resonant devices.

Among the numerous methods that exist for finding approximate solutions to the field problem in various devices [1], there are some that offer greater accuracy when determining resonant frequencies and other characteristic parameters, an accuracy which today is a technological necessity (e.g. satellite communications). Among these sophisticated methods we can mention those based on a dielectric waveguide model [2]–[4], a mixture of the magnetic wall and dielectric waveguide models [5], finite elements [6], a variational method [7]–[9], and, lastly, Green's function techniques [10], which are very powerful given that they can be applied to very different situations.

With regard to the Green's function methods, those which incorporate the free-space Green's function and which are based on a surface integral approach stand out for their simplicity. Usually these methods consider bound systems and use equivalent currents as a starting point (Glisson and Kajfez [10]). The method presented in this paper is based on Kirchhoff's integral formulation with the free-space Green's function (field components are the basic entities involved) and allows the approximate study of unbound systems.

Manuscript received March 21, 1988; revised May 1, 1989.
The authors are with the Departamento de Física Aplicada, Facultad de Ciencias, Universidad de Murcia, 30071 Murcia, Spain.
IEEE Log Number 8930651.

II. Numerical Method

Fig. 1 shows the kind of systems which we are interested in. They are composed of different lossless homogeneous regions with axial symmetry along the Z axis. This symmetry allows special modes to be defined, which correspond to diverse (and usually complex) resonance frequencies of the structure and whose components (in cylindrical coordinates (r, θ, z) associated to the system) would be as follows:

$$f(r,z)\cdot[a\cos(p\theta)\pm b\sin(p\theta)], \qquad p=0,1,2,\cdots. \quad (1)$$

For each mode we use Kirchhoff's integral equation in every dielectric region of the structure and integrate with respect to the angular variable, θ, (taking points $\boldsymbol{r}$ in the half-plane $\theta=0$ (Fig. 1)). This results in a line integral equation extending to the boundary L ($\theta=0$) of the considered region involving only the $f(r,z)$ part of each field component:

$$\frac{\Omega(\boldsymbol{r})}{4\pi}\psi(\boldsymbol{r})=\int_L A(\boldsymbol{r},l')\varphi(l')\,dl' \quad (2)$$

where

$$\psi(\boldsymbol{r})=\begin{bmatrix}|e_r|\\|h_r|\\|e_\theta|\\|h_\theta|\\|e_z|\\|h_z|\end{bmatrix} \qquad \varphi(l')=\begin{bmatrix}|e_\theta|\\|h_\theta|\\|e_l|\\|h_l|\end{bmatrix}$$

$$A(\boldsymbol{r},l')=\begin{bmatrix}A^{r\theta} & A^{rl}\\ A^{\theta\theta} & A^{\theta l}\\ A^{z\theta} & A^{zl}\end{bmatrix} \quad (3)$$

TABLE I
EXPRESSION OF COEFFICIENT MATRIX $A^{\alpha\beta}$

$$A_{11}^{r\theta} = [n_r \cdot r' + n_z \cdot (z' - z)] \cdot I_3'$$

$$A_{12}^{r\theta}(\mu,\epsilon) = J\{-w_c\mu n_z I_2 + \frac{1}{w_c\epsilon}[I_2' \cdot (n_z - r' \frac{\partial}{\partial l'}) - rI_1'](\frac{n_z}{r'} + \frac{\partial}{\partial l'})\}$$

$$A_{11}^{rl} = (z' - z) \cdot I_2'$$

$$A_{12}^{rl}(\mu,\epsilon) = J \cdot [w_c\mu I_3 + \frac{p}{w_c\epsilon}(I_2' - \frac{r}{r'} \cdot I_1')]$$

$$A_{11}^{\theta\theta} = n_r r I_1' - [n_r r' + n_z (z' - z)] I_2'$$

$$A_{12}^{\theta\theta}(\mu,\epsilon) = J \cdot [w_c\mu n_z I_3' - \frac{I_3'}{w_c\epsilon}(n_z - r' \frac{\partial}{\partial l'})]$$

$$A_{11}^{\theta l} = -(z' - z)\, I_3' \qquad A_{12}^{\theta l}(\mu,\epsilon) = -J[w_c\mu I_2 + \frac{p}{w_c\epsilon} \cdot I_3']$$

$$A_{11}^{z\theta} = -n_z r I_3'$$

$$A_{12}^{z\theta}(\mu,\epsilon) = J\{w_c\mu n_r I_1 + \frac{I_1'}{w_c\epsilon}[n_z \frac{z'-z}{r'} - (z'-z) \cdot \frac{\partial}{\partial l'}]\}$$

$$A_{11}^{zl} = -(r' I_1' - r I_2') \qquad A_{12}^{zl}(\epsilon) = J \frac{p}{w_c\epsilon r'} \cdot (z'-z) \cdot I_1'$$

$$A_{22}^{\alpha\beta} = K \cdot A_{11}^{\alpha\beta} \qquad K = \begin{cases} 1 & \alpha\beta = rl,\ \theta\theta,\ zl \\ -1 & \text{otherwise} \end{cases}$$

$$A_{21}^{\alpha\beta} = K' \cdot A_{12}^{\alpha\beta} \qquad K' = \begin{cases} 1 & \alpha\beta = rl,\ zl \\ -1 & \text{otherwise} \end{cases}$$

where:

$$\begin{bmatrix} I_1 \\ I_2 \\ I_3 \end{bmatrix} = 2r' \int_0^{\pi} G \cdot \cos(\theta) \cdot \begin{bmatrix} 1 \\ \cos(p\theta) \\ \sin(p\theta) \end{bmatrix} d\theta \ ; \ G = \frac{e^{-jkR}}{4\pi R} \ ; \ R = |r' - r|$$

$$\begin{bmatrix} I_1' \\ I_2' \\ I_3' \end{bmatrix} = 2r' \int_0^{\pi} \frac{G'}{R} \cdot \cos(\theta) \cdot \begin{bmatrix} 1 \\ \cos(p\theta) \\ \sin(p\theta) \end{bmatrix} d\theta \ ; \ G' = \frac{dG}{dR} \ ; \ \hat{n} = (n_r, 0, n_z)$$

are, respectively, the whole field in r, its θ and l components at a point l' of the boundary and a $A_{6\times4}$ coefficient matrix (see Table I). These depend on the medium's geometry, their electromagnetic characteristics (ϵ, μ), the frequency ω_c, and the mode parameter p.

Equation (2) is solved by using a moment method technique. The boundary L is divided into N intervals, Δ_j (see Fig. 1), centered on the N points Q_j $(j = 1,2,\cdots,N)$. The fields in the boundary $\varphi(l')$ can be approximated by a linear combination of pulse functions defined on the intervals Δ_j.

Then, a point matching technique is used, on the N points Q_j, by considering the different homogeneous dielectric regions of the structure with its coupling boundary conditions. The following system of equations is obtained:

$$\sum_{j=1}^{M} B_{i,j}(\omega_c) X_j = 0, \qquad i = 1,\cdots,M \tag{4}$$

where X_j represents all the unknown coefficients associated with the fields in all the boundaries involved.

The solution of the homogeneous system of equations (4) determines the frequency spectrum, ω_c, and the coefficients X_j of the field components e_θ, h_θ, e_l, and h_l in the boundaries. When these coefficients are known, (2) can be used to calculate the field components at any point r in the system.

III. APPLICATIONS

In order to verify the effectiveness of the described method, we present some of the results corresponding to the analysis of two systems which allow a simple analytical contrast: a) a dielectric-loaded metallic cavity and b) a short-circuited dielectric resonator (for trapped modes) [12]. Through these the most noticeable aspects in applying the method can be seen.

TABLE II
THEORETICAL AND CALCULATED RESONANT FREQUENCIES (k_0 R) FOR SEVERAL MODES OF (a) A DIELECTRIC-LOADED CAVITY (STRUCTURE AS IN FIG. 2(a)) $R = 22.5$ mm, $L = 39$ mm, $T = 19.5$ mm, $\epsilon_r = 10$) AND (b) A CYLINDRICAL DIELECTRIC RESONATOR SHORT-CIRCUITED AT BOTH ENDS BY PARALLEL CONDUCTING PLATES (STRUCTURE AS IN FIG. 2(b)) $R = 7$ mm, $L = 7.5$ mm, $\epsilon_r = 35$)

mode	k_0R	
	theor.	calcul.
TM_{011}	0.935	0.953
TE_{111}	0.987	0.976
TM_{111}	1.333	1.323
TE_{011}	1.509	1.508
TM_{012}	1.768	1.768
TE_{112}	1.882	1.867
TM_{112}	2.056	2.013
TE_{012}	2.249	2.241
TE_{013}	3.190	3.180

(a)

mode	k_0R	
	theor.	calcul.
HEM_{111}	0.620	0.628
TE_{011}	0.712	0.712
TM_{011}	0.810	0.813
HEM_{121}	0.877	0.895
HEM_{131}	1.030	1.047
HEM_{112}	1.062	1.052
TE_{021}	1.111	1.110
TE_{012}	1.138	1.135
TM_{012}	1.182	1.183
HEM_{0122}	1.258	1.240
TM_{021}	1.272	1.274

(b)

Table II shows the numerical values obtained for the parameter k_0R, where $k_0^2 = \omega^2\epsilon_0\mu_0$, for different modes in the two systems. In Fig. 2 we present the fields within the boundaries for some of the modes appearing in Table II. The boundaries of the systems are divided into (a) 44 and (b) 15 intervals.

As can be appreciated, with a moderate discretization the results are generally quite accurate, with an error in the frequency less than or on the order of 1 percent.

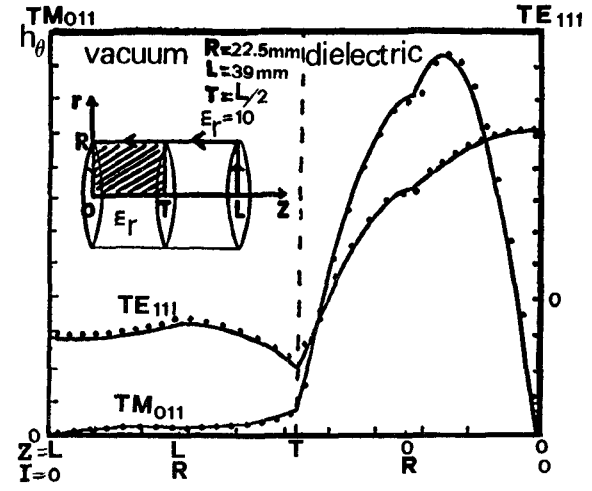

(a)

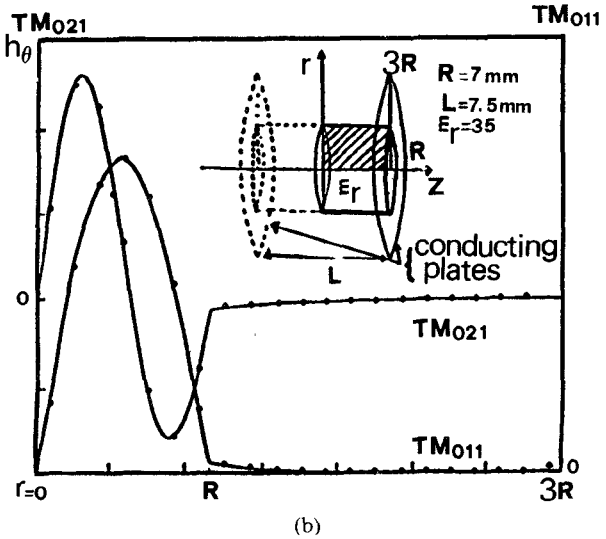

(b)

Fig. 2. The distribution of the h_θ field component at the metallic surface for (a) the TM_{011} and TE_{111} modes on dielectric-loaded cavity and (b) the TM_{011} and TM_{021} modes on shielded dielectric resonator.

IV. Conclusions

The numerical results obtained in studying several systems confirm the validity of the method and its wide fields of applications. Theoretically it is worth noting the simplicity and generality of the formulation, which allow such problems as unbound systems to be tackled, something that is difficult with other techniques. The complexity of the numerical procedure is not excessive and the consideration of a low number of intervals in the boundary partition leads to quite accurate results (errors in frequency being less than 1 percent).

References

[1] D. Kajfez and P. Guillon, Eds., *Dielectric Resonators*. Norwood, MA. Artech House, 1986.

[2] J. Krupka, "Computations of frequencies and intrinsic Q factors of TE_{0nm} modes of dielectric resonators," *IEEE Trans. Microwave Theory Tech.*, vol. MTT-33, pp. 274–277, Mar. 1985.

[3] M. W. Pospieszalski, "Cylindrical dielectric resonators and their applications in TEM line microwave circuits," *IEEE Trans. Microwave Theory Tech.*, vol MTT-27, pp. 233–238, Mar. 1979.

[4] T. Itoh and R. Rudokas, "New method for computing the resonant frequency of dielectric resonator," *IEEE Trans Microwave Theory Tech.*, vol. MTT-25, pp. 52–54, Jan. 1977.

[5] Y. Garault and P Guillon, "Higher accuracy for the resonance frequencies of dielectric resonators," *Electron. Lett*, vol 12, pp. 475–476, Sept. 1976.

[6] P S Kooi, M. S Leong, and A L. Satya Prakash, "Finite-element analysis of the shielded cylindrical dielectric resonator," *Proc Inst Elec Eng.*, vol. 132, pp 7–16, Feb 1985.

[7] J. Van Bladel, "On the resonances of dielectric resonator of very high permittivity," *IEEE Trans Microwave Theory Tech.*, vol. MTT-23, pp. 199–208, Feb. 1975.

[8] Y. Konishi, N Hoshino, and Y. Utzumi, "Resonant frequency of a $TE_{01\delta}$ dielectric resonator," *IEEE Trans. Microwave Theory Tech.*, vol. MTT-24, pp. 112–114, Feb 1976.

[9] M. Jaworski and M. W. Pospieszalski, "An accurate solution of the cylindrical dielectric resonator problem," *IEEE Trans. Microwave Theory Tech*, vol. MTT-27, pp 639–643, July 1979

[10] A. W Glisson, D. Kajfez, and J James, "Evaluations of modes in dielectric resonators using a surface integral equation formulation," *IEEE Trans. Microwave Theory Tech*, vol MTT-31, pp. 1023–1029, Dec. 1983

[11] R. F. Harrington, *Field Computations by Moment Method* New York: Macmillan, 1968.

[12] Y Kobayashi and S Tanaka, "Resonant modes of a dielectric rod resonator short-circuited at both ends by parallel conducting plates," *IEEE Trans. Microwave Theory Tech*, vol. MTT-28, pp. 1077–1084, Oct. 1980.

An Experimental Investigation of the Microstrip Step Discontinuity

JAMES C. RAUTIO, MEMBER, IEEE

Abstract—**Measurements of a cascade of microstrip step discontinuities are compared with results of an electromagnetic analysis and with models available in commercial software. The experimental validation technique, which can be applied to other discontinuities, is described.**

I. Introduction

This paper describes a broad-band validation technique as applied to a step discontinuity. The technique was developed for the validation of the electromagnetic (em) analysis [1]–[3].

While there are many results for the step, most [4]–[11], [17]–[19] specify non-50-Ω S parameters. Since the normalizing impedances, which allow conversion to 50 Ω (especially in regard to reflection phase), are rarely specified, it is difficult to compare results. Instead, we compare with the 50-Ω S parameters provided by most commercial models.

Koster and Jansen [4] state that measurement of the step "seems hardly feasible with the present state-of-the-art," as the discontinuity effect is small at low frequencies (where accurate measurements are possible) and is difficult to measure at high frequencies. Many validation attempts involve measurement of a single discontinuity at high frequency, resulting in an undesirably large scatter [8]–[14].

Resonance techniques [23] are especially suited to non-50-Ω modeling and could have been applied in the above cases. The technique is useful for generating low-loss two-port discontinuity models. The technique described here is applicable to lossy and multiport validation but not for generating models or for non-50-Ω systems. Our results suggest that the reflection phase of a

Manuscript received August 1, 1988; revised July 7, 1989

The author is with Sonnet Software, Inc., 4397 Luna Course, Liverpool, NY 13090.

IEEE Log Number 8930654.